Hydrodynamic and Spectral Simulations of HMXB Winds

aka "Physics of Wind-fed Accretion"

Christopher W. Mauche

Duane A. Liedahl

Lawrence Livermore National Laboratory

Shizuka Akiyama

LLNL / KIPAC, Stanford University

Tomasz Plewa

University of Chicago / Florida State University

Cool Discs, Hot Flows • March 25–30, 2008 • Funäsdalen, Sweden

In detached HMXBs, the neutron star accretes a small fraction of the stellar wind of the massive OB star

Mass accretion rate: $\dot{M}_a = \pi r_a^2 \rho v_{\rm rel}$, where

- Accretion cylinder radius: $r_a = \xi 2GM_x/v_{\rm rel}^2 =$ $2.7\times10^{10}\, \xi\, (M_x/M_\odot)\, (v_{\rm rel}/10^3 \text{ km/s})^{-2}$ cm,
- Relative velocity: $v_{\rm rel} = (v_w^2+v_x^2)^{1/2}$; $v_{\rm rel}/v_w = [1+(v_x/v_w)^2]^{1/2}$
- Wind density: $\rho = \dot{M}_w/4\pi a^2 v_w$, hence:

$$\dot{M}_a = 1/4\, (r_a/a)^2\, (v_{\rm rel}/v_w)\, \dot{M}_w = 2.6\times10^{-4}\, \dot{M}_w = 3.4\times10^{-10}\, \xi^2\, (v_w/v_{\rm esc})^{-4}\, (M_x/1.86\, M_\odot)^2\, (M_*/23.8\, M_\odot)^{-8/3}\, (R_*/30\, R_\odot)^2\, (P/8.96\text{ d})^{-4/3}\, (\dot{M}_w/10^{-6}\, M_\odot/\text{yr})\, M_\odot/\text{yr},$$

where $v_{\rm esc} = (2GM_*/R_*)^{1/2} = 550$ km/s and $v_w/v_{\rm esc} = 3/2$

X-ray luminosity: $L_x = GM_x\dot{M}_a/R_x = 5.2\times10^{36}$ erg/s

Hoyle & Lyttleton (1939), Shapiro & Lightman (1976)

The wind of an isolated OB star is driven by radiation pressure on line opacity that overlaps with the stellar spectrum

Castor, Abbot, & Klein (1975): “CAK”

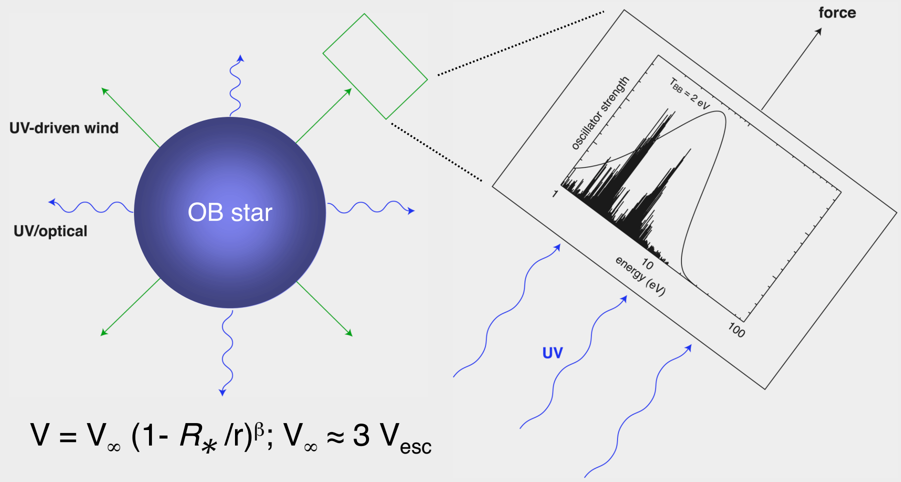

$V = V_\infty\,(1 - R_* / r)^\beta;\ V_\infty \approx 3\,V_{esc}$

In an HMXB, X-ray photoionization destroys the important sources of UV line opacity, significantly reducing the radiative driving of the wind

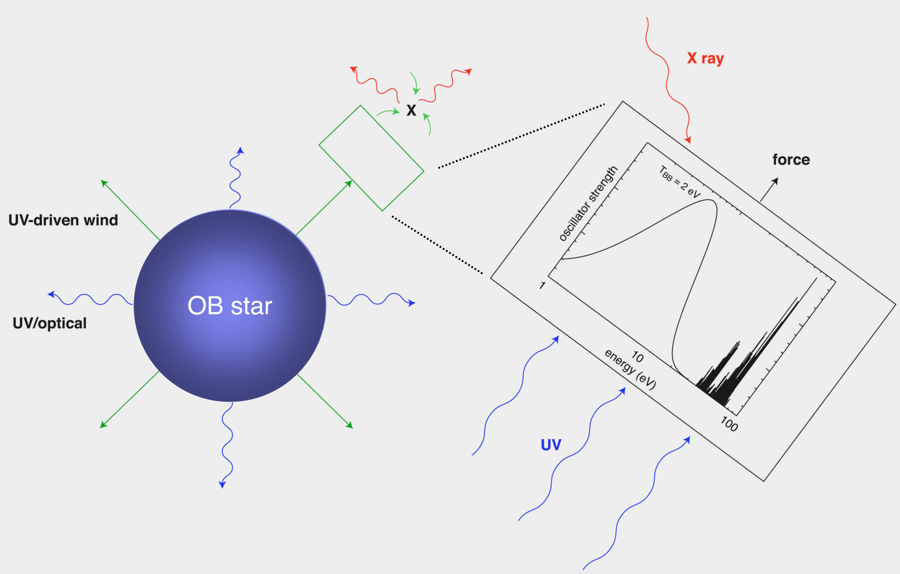

Despite these complications, the L_X~5x10^{36} erg s^{-1} of Vela X-1 is consistent with accretion onto the neutron star from the wind of the B0.5 Ib supergiant

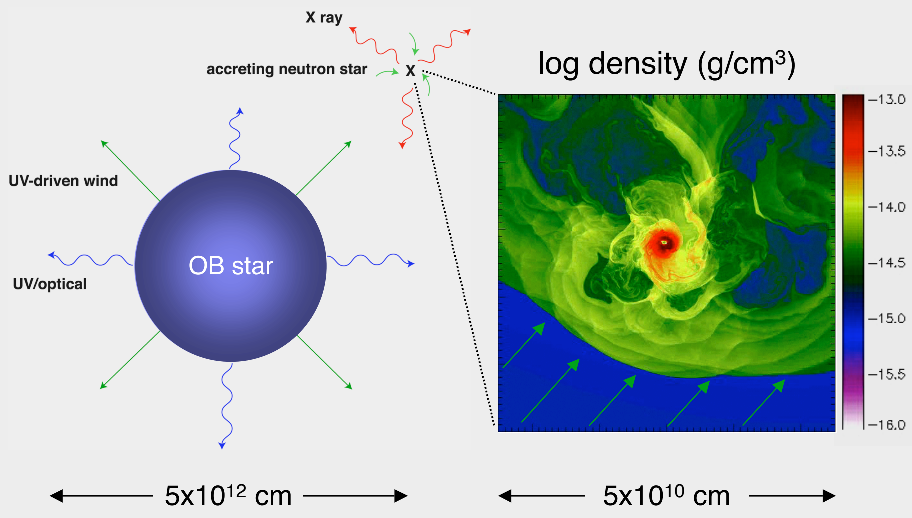

Using *ASCA* data, Nagase et al. (1994) demonstrated that the eclipse spectrum of Vela X-1 is dominated by emission lines of He-like Ne, Mg, Si, … Fe

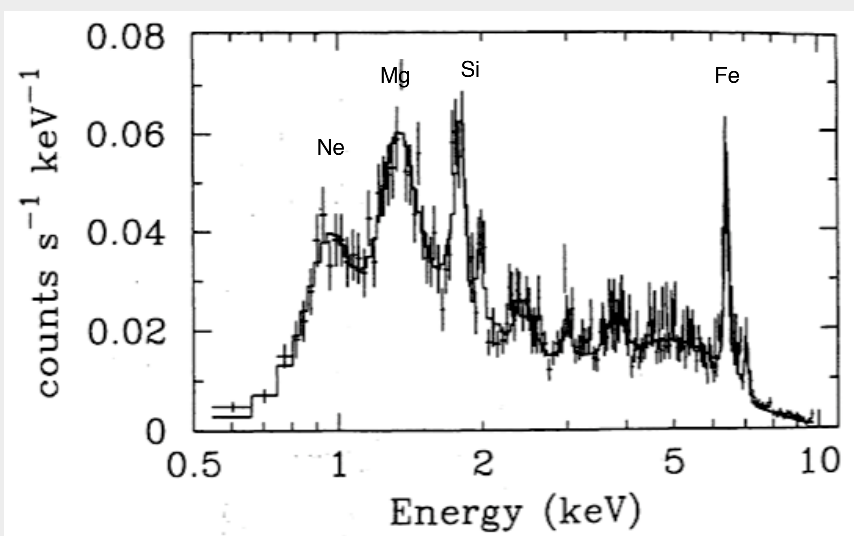

Sako et al. (1999) analyzed the *ASCA* spectrum of Vela X-1 in eclipse using the DEM distribution of a generalized (but otherwise unperturbed) CAK wind

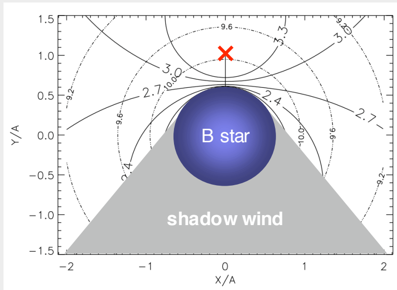

L_x
$\dot{M}$
V_∞
β

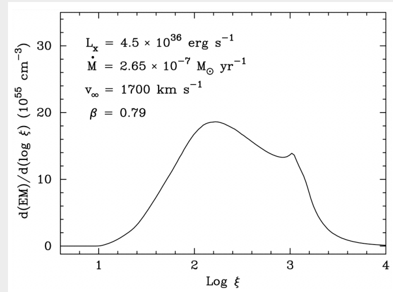

$$\xi = L_x / nR^2$$
$$n = \dot{M}/4\pi\mu V r^2$$
$$V = V_\infty(1 - R_*/r)^\beta$$

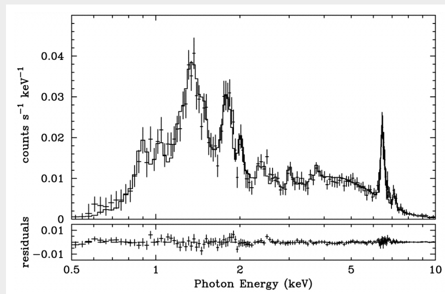

Using similar assumptions and a MC simulator, Watanabe et al. (2006) modeled the *Chandra* HETG spectra of Vela X-1 at three orbital phases

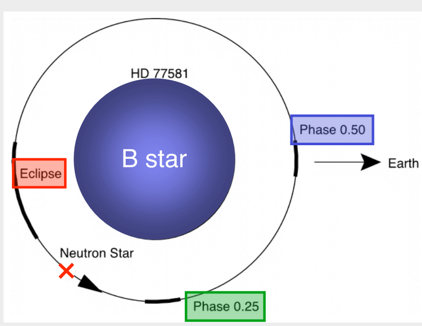

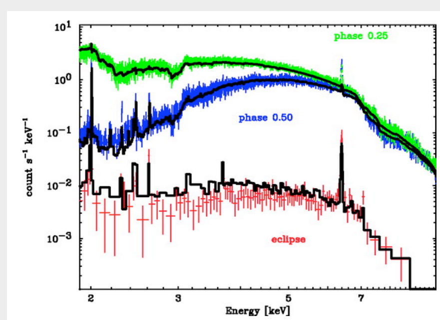

Assuming canonical values for L_x, V_∞, and β, Watanabe et al. derived $\dot{M}$ = 1.5–2x10^{-6} $M_\odot$/yr (~ 6 times that of Sako et al. 1999 [??]).

To account for the affects of photoionization, Watanabe et al. conducted a 1-D calculation to estimate the wind velocity along the line of centers

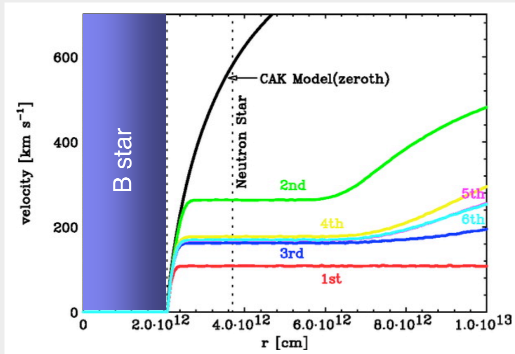

Watanabe et al. found that photoionization reduces the stellar wind velocity by a factor of 2–3 near the neutron star, in good agreement with observations.

Blondin et al. (1990–1995), using 2- and 3-D hydrodynamic calculations, showed that wind accretion in HMXBs is far more complex …

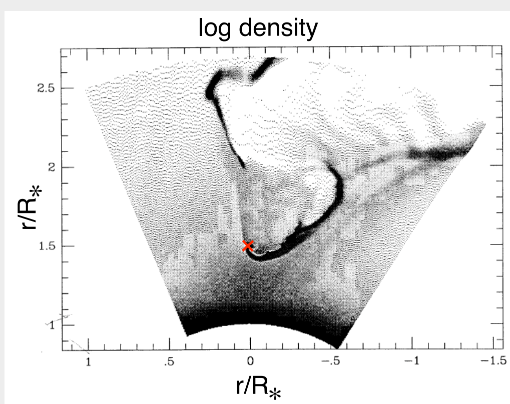

Models were used primarily to model/interpret the binary phase-dependent photoelectric absorption.

Level of detail present in the *Chandra* HETG spectra demands that we construct detailed models that account for all the relevant physical process

Detail of *Chandra* spectrum of Vela X-1 in eclipse

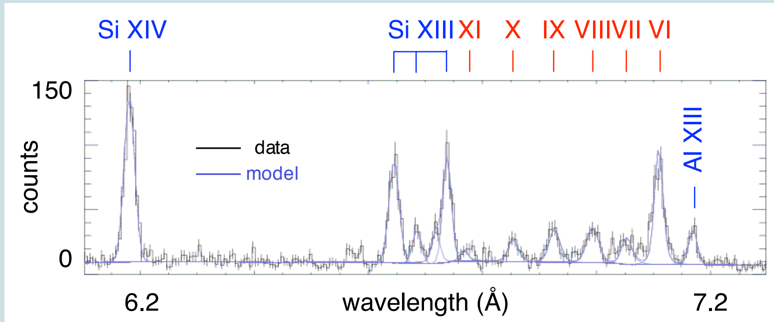

Features to match are the continuum and line intensities and the widths and shifts of the lines, *all as a function of binary phase.*

To account for this complexity, we are developing a 3-D radiation hydrodynamic model of the winds of HMXBs

The model includes:

- **XSTAR** photoionization calculations: $f_{ij}(\xi, T)$, Γ, Λ
- **HULLAC** atomic models:
  - Improved calculations of the radiative force multiplier *M*
  - X-ray emission models for X-ray photoionized plasmas
- **FLASH** AMR hydrodynamic calculations including:
  - gravity
  - rotation
  - Compton and photoionization heating Γ,
  - Compton and radiative cooling Λ, and
  - radiative acceleration for X-ray photoionized plasmas
- **Monte Carlo** radiation transport

Radiative driving of the wind is accounted for via the force multiplier formalism (Castor, Abbott, & Klein 1975)

Force multiplier M is determined on a 3-D lattice (T, ξ, t – 21x51x41)

Force multiplier for selected ions

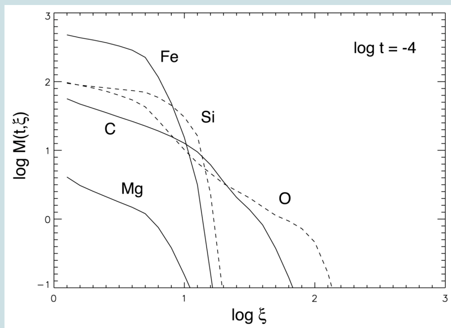

$$F_{rad} = F_{elec}\ (1+M)$$

$$M = \Sigma\ \Delta\nu\ (F_\nu/F)\ (1-e^{-\eta t})\ /\ t$$

$$t = \rho \kappa_e v_{th} (dv/dr)^{-1}$$

η: atomic physics:

HULLAC models:
- 166 ions of 13 elements
- 35,000 energy levels
- 2,000,000 atomic lines (visible – X-ray)
- explicit level populations

Our detailed non-LTE treatment of atomic physics improves on the current standard calculation of radiative driving (Stevens & Kallman 1990)

Comparison with Stevens & Kallman

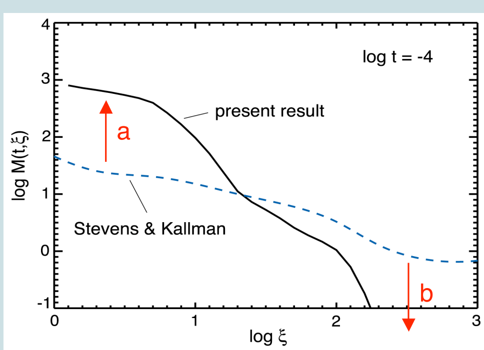

HULLAC models:
- 13 elements
- 166 ions
- 35,000 energy levels
- 2,000,000 atomic lines (visible – X-ray)
- explicit level population solutions

a: more detailed atomic models
b: do not assume LTE

Our revised force multiplier alters the radiative driving of the wind, the resulting hydrodynamics, and hence the emitted X-ray spectrum.

FLASH models will (do not yet) account for the reduction in the radiative driving due to finite wind optical depth

Spectral breakdown of Si II force multiplier for different *t*

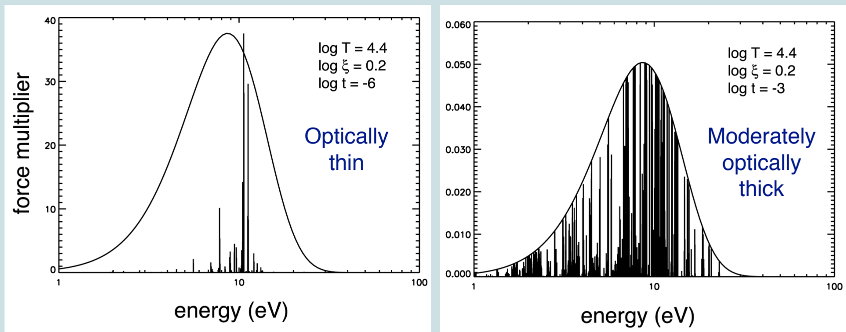

Line saturation reduces the radiative driving, dramatically affecting the wind dynamics.

FLASH simulations result in time-varying spatial maps of temperature *T*, density *n*, velocity *v*, and ionization parameter ξ

2-D FLASH simulation of Vela X-1

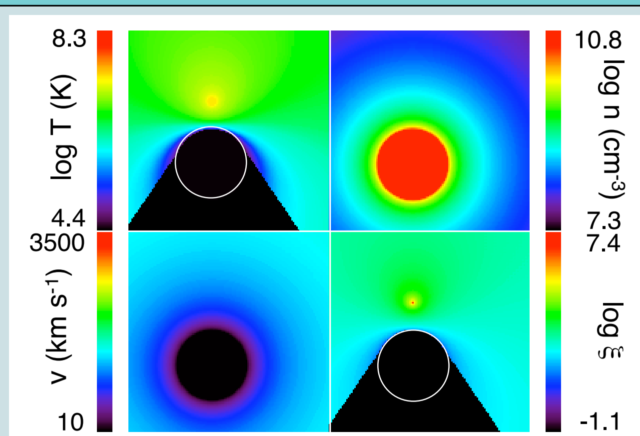

Asymmetries affect the predicted X-ray spectrum in ways that cannot be captured by simple models.

FLASH simulations result in time-varying spatial maps of temperature *T*, density *n*, velocity *v*, and ionization parameter ξ

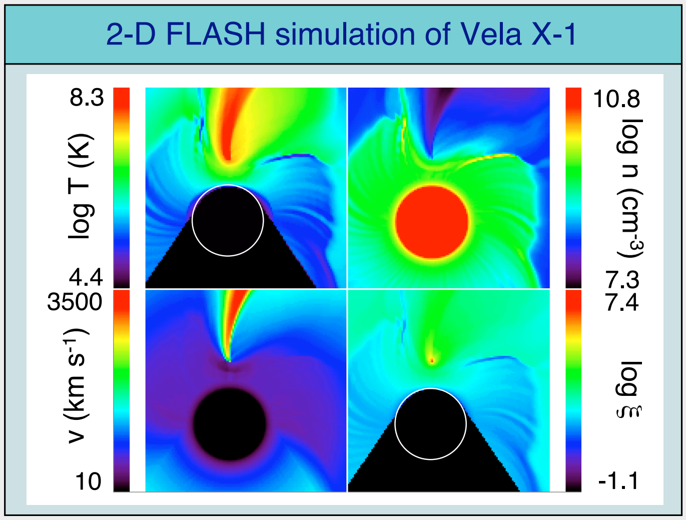

Asymmetries affect the predicted X-ray spectrum in ways that cannot be captured by simple models.

Physical quantities can be used to produce maps of the emissivity distributions in various emission lines

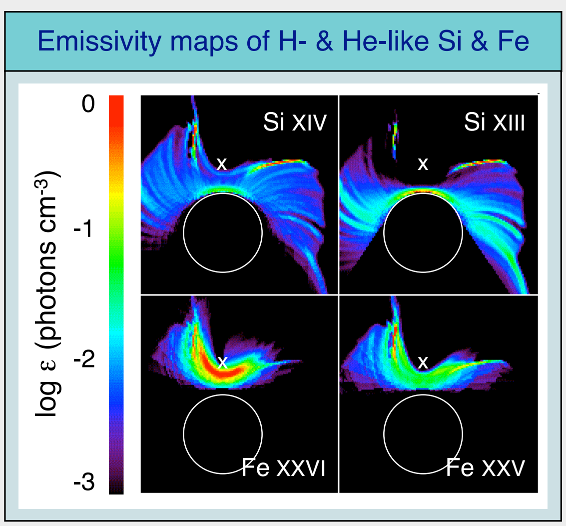

Emissivity maps constrain the location of the emission regions via the binary-phase dependence of the X-ray spectra.

FLASH 3-D simulations are being run to produce the required 3-D grids of temperature *T*, density *n*, velocity *v*, and ionization parameter ξ

3-D FLASH simulation of Vela X-1

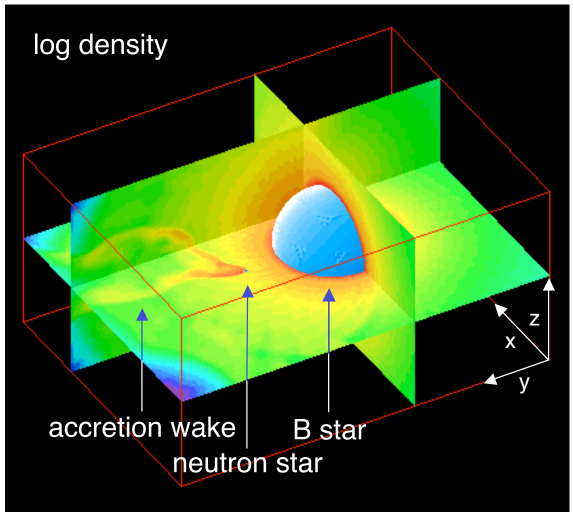

FLASH 3-D simulations are being run to produce the required 3-D grids of temperature *T*, density *n*, velocity *v*, and ionization parameter ξ

3-D FLASH simulation of Vela X-1

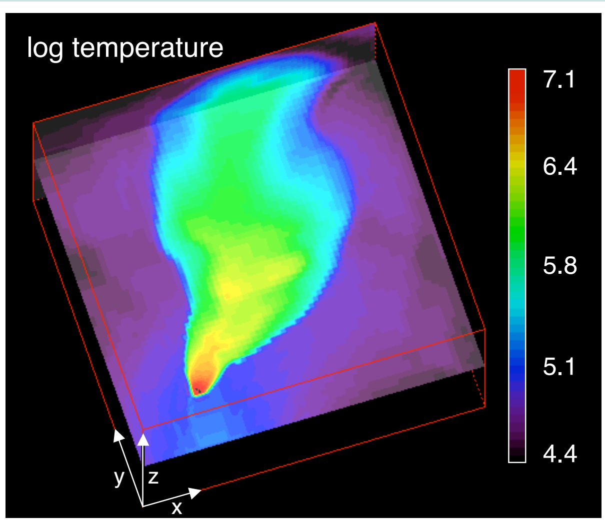

Resolution study of the accretion flow in the vicinity of the neutron star. The level of refinement varies from 7 to 15 (from ~8x10⁹ to 3x10⁷ cm)

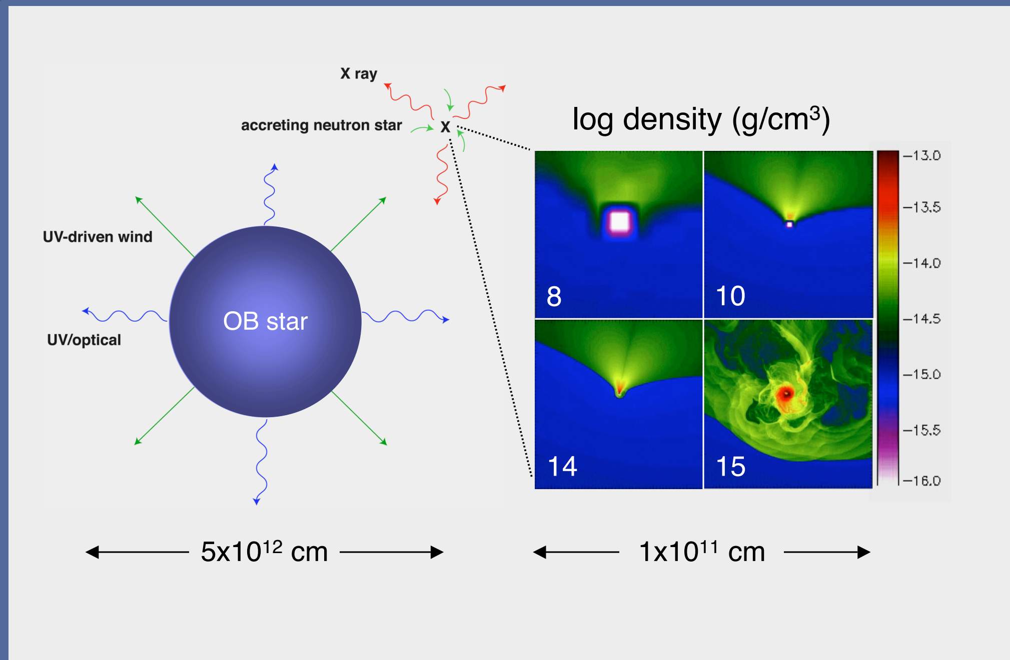

Resolution study of the accretion flow in the vicinity of the neutron star. The level of refinement varies from 7 to 15 (from ~7x10⁹ to 3x10⁷ cm)

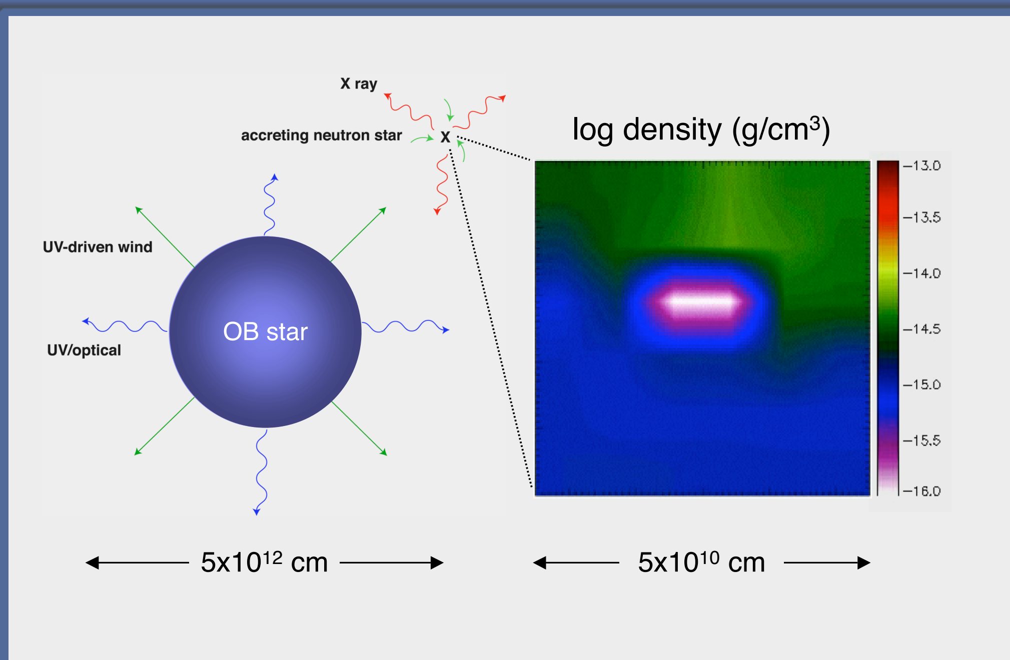

The FLASH 3-D grids of T, n, v, and ξ are fed into our* Monte Carlo radiation transfer code to produce synthetic X-ray spectral models

The Monte Carlo code accounts for:

- Continuum opacity for 446 subshells of 140 ions of the 12 most abundant elements
- RRC and recombination line cascades following photo-absorption by K-shell ions
- Fluorescent line emission following inner-shell photo-absorption by M-shell ions
- Compton scattering
- Line scattering with partial redistribution
- Doppler shifts due to the velocity field

*Mauche, Liedahl, Mathiesen, Jimenez-Garate, & Raymond (2004, ApJ)

Preliminary results of the Monte Carlo code show dramatic differences between an unmodified CAK wind model and a full-up 3D FLASH model

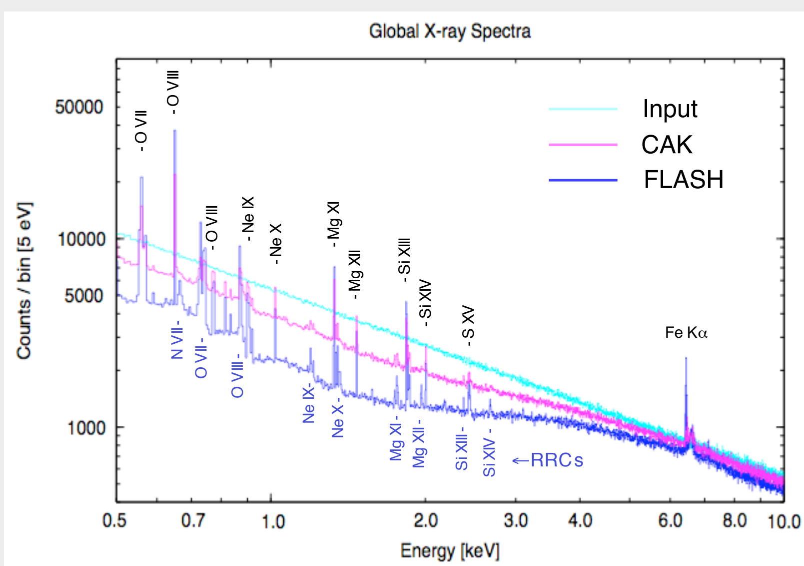

Recall that the *Chandra* HETG spectrum of Vela X-1 showed strong lines of L-shell ions of Si

Detail of *Chandra* spectrum of Vela X-1 in eclipse

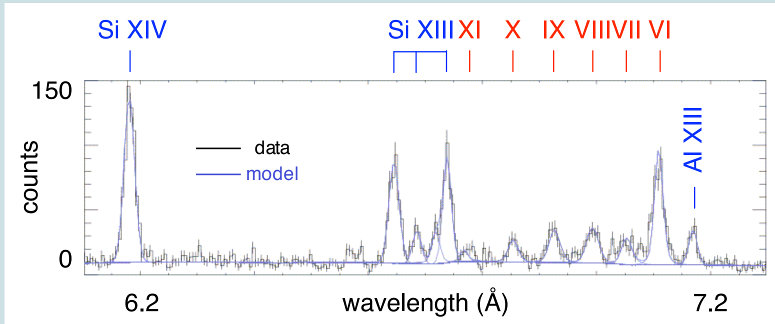

How can this be, given (so the common wisdom is) that such lines are strongly suppressed by resonant Auger destruction?

Resonant Auger Destruction (RAD) leads to the suppression of Kα lines of L-shell ions (Liedahl 2005)

Fluorescence:

$\varepsilon + A_{i-1}$	$\rightarrow A_i^{**} + e^-$	K-shell photoionization
A_i^{**}	$\rightarrow A_{i+1} + e^-$	Autoionization (Auger effect)
	$\rightarrow A_i^{*} + \varepsilon_K$	Spontaneous radiative decay

Resonant Auger Destruction (RAD):

$\varepsilon_K + A_i^{*}$	$\rightarrow A_i^{**}$	Resonant absorption*
A_i^{**}	$\rightarrow A_{i+1} + e^-$	Auger decay - photon destruction

Net effect is the suppression of Kα lines of L-shell ions

*optical depth $\tau_{lu} = N_H A_Z F_{ion} p_l (\pi e^2/mc) f_{lu} \varphi(\upsilon)$

level populations p_l are affected by the radiation field

Be-like Fe XXIV spectrum with and without photoexcitation by a dilute 80 eV blackbody radiation field

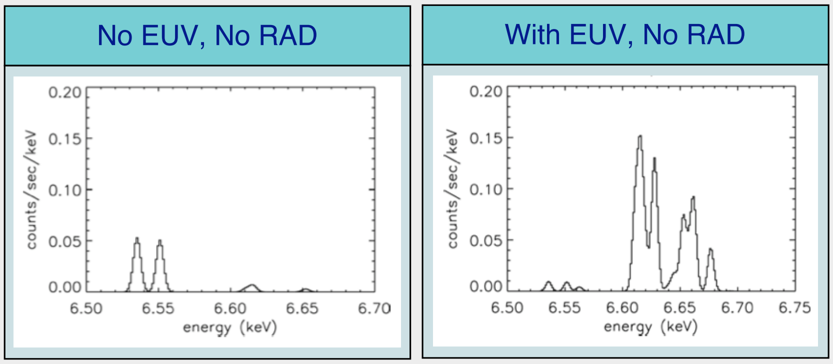

Even without RAD, a dilute radiation field affects the level populations and hence the observed spectrum; in this case, the lines are brighter (higher in yield) and higher in energy.

The dramatic effect of the EUV radiation field on the Be-like Fe XXIV spectrum is due to the depletion of the ground-state population

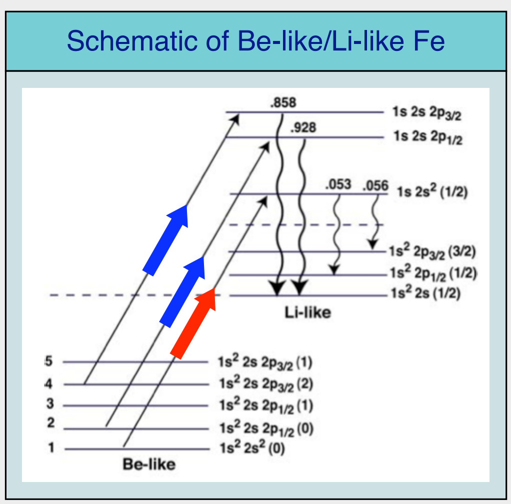

Kα lines for transitions out of the ground/excited state have lower/higher fluorescence yields and lower/higher energies.

Accounting for both photoexcitation and RAD, the observed Kα spectrum is a function of the ion column density

Fe XXIV spectra for 4 ionic column densities

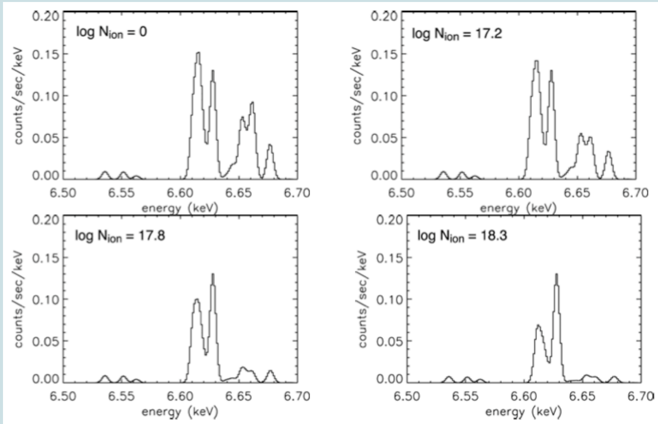

Accounting for photoexcitation, the effective Kα yield of Be-like Fe XXIV is nonzero for even moderately high ionic column densities.

The effective Kα yields of L-shell Fe is everywhere greater with photo-excitation than without

Fluorescent yields vs. ionic column density

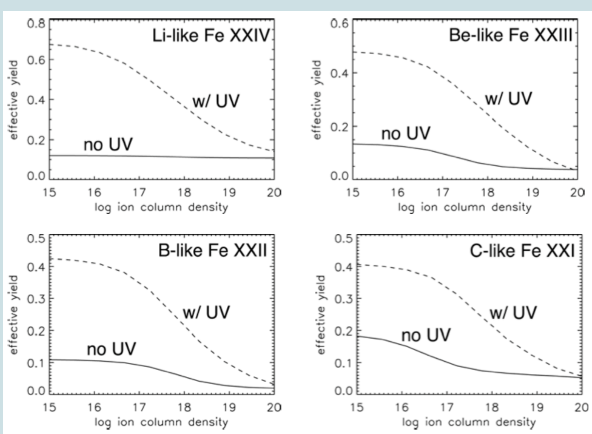

This behavior casts doubt on the common practice of zeroing out the Kα lines of L-shell ions.

We have begun full-up Monte Carlo calculations of RAD, including all the relevant physical processes…

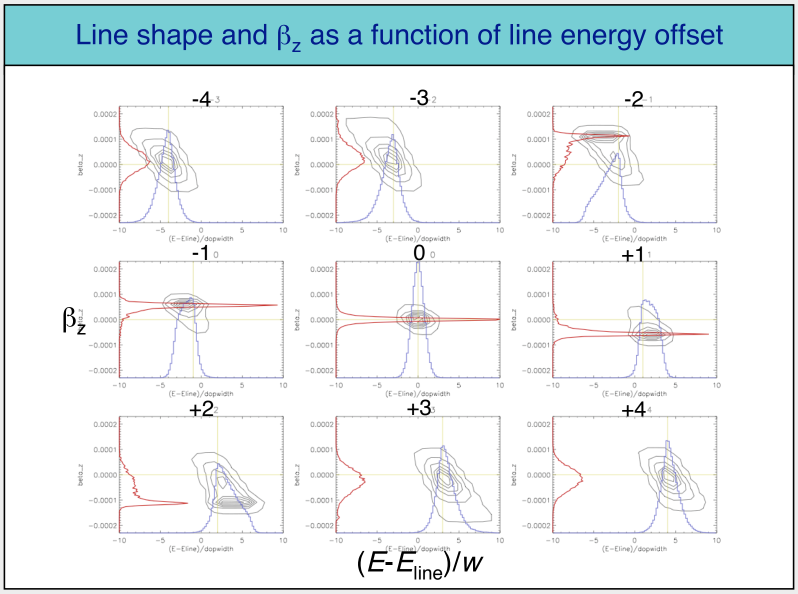

We are using FLASH hydrodynamic simulations, HULLAC atomic models, and Monte Carlo radiation transfer to model the X-ray spectra of HMXBs

FLASH Hydrodynamic Simulations

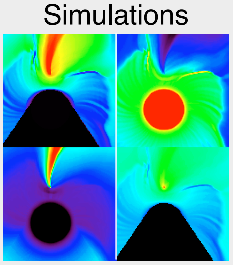

+

HULLAC Atomic Models & Monte Carlo Radiation Transfer

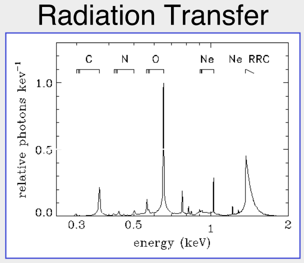

+

High-Resolution X-ray Spectra (*Chandra, XMM*)

Theoretical spectra

Observed spectra

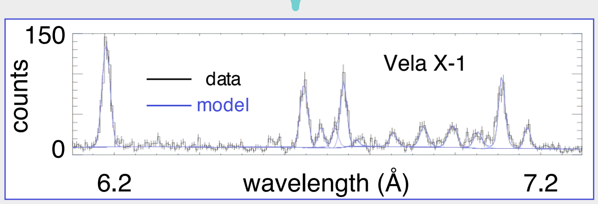

Acknowledgements

This work was performed under the auspices of the U.S. Department of Energy by Lawrence Livermore National Laboratory under Contract DE-AC52-07NA27344. This work was funded by the Laboratory Directed Research and Development Program at LLNL under project tracking code 05-ERD-044. T. Plewa's contribution to this work was supported in part by the U.S. Department of Energy under Grant No. B523820 to the Center for Astrophysical Thermonuclear Flashes at the University of Chicago. The FLASH software used in this work was developed in part by the DOE-supported ASC/Alliance Center for Astrophysical Thermonuclear Flashes at the University of Chicago.

Physical Sciences

Acknowledgements

This work was performed under the auspices of the U.S. Department of Energy by Lawrence Livermore National Laboratory under Contract DE-AC52-07NA27344. This work was funded by the Laboratory Directed Research and Development Program at LLNL under project tracking code 05-ERD-044. T. Plewa's contribution to this work was supported in part by the U.S. Department of Energy under Grant No. B523820 to the Center for Astrophysical Thermonuclear Flashes at the University of Chicago. The FLASH software used in this work was developed in part by the DOE-supported ASC/Alliance Center for Astrophysical Thermonuclear Flashes at the University of Chicago.

Physical Sciences